

23.5 An Energy Pile-Up Resonance Circuit Extracting Maximum 422% Energy from Piezoelectric Material in a Dual-Source Energy-Harvesting Interface

Young-Sub Yuk, Seungchul Jung, Hui-Dong Gwon, Sukhwan Choi, Si Duk Sung, Tae-Hwang Kong, Sung-Wan Hong, Jun-Han Choi, Min-Yong Jeong, Jong-Pil Im, Seung-Tak Ryu, Gyu-Hyeong Cho

KAIST, Daejeon, Korea

Energy harvesting is one of the key technologies used to realize self-sustaining systems such as wireless sensor networks and health-care devices. Much research on circuit design has been conducted to extract as much energy as possible from transducers, such as the *thermoelectric generator (TEG)* and the *piezoelectric transducer (PZT)*. Specifically, the energy in a PZT could be extracted more efficiently by utilizing resonance as [1] and [2] demonstrated. However, the maximum output voltage swing in those techniques are limited to twice of the original swing of the PZT, and thus, had a limited energy extraction capability in spite of more energy being available from the PZT. In [3], on the other hand, the large energy is obtained with higher voltage swing, but is limited up to 247% because the load energy is used to increase the output voltage swing of PZT. To obtain far more power from PZT, we propose an alternative resonance technique through which the PZT output swing can be boosted as high as CMOS devices can sustain. This technique is applied to a dual-energy- sourced (PZT and TEG) *energy-harvesting interface (EHI)* as a battery charger.

In Fig. 23.5.1, the equivalent electric model having dual energy sources, PZT and TEG, is shown with the detailed schematic of the proposed EHI. This circuit harvests energy from the TEG by a conventional boost converter operation through paths I and III in *discrete current mode (DCM)*, where the TEG generates 500mV for a temperature difference of about 10°K. The energy from the PZT is harvested through paths II and III simultaneously with the energy in the TEG by time multiplexing. The utilized PZT generates a peak AC power at 100Hz. Since the AC frequency of the PZT is low, the operational frequency of the boost converter is set at 2.5kHz.

Two waveforms are illustrated in the Fig. 23.5.2. Normally, the amount of energy extraction from the PZT is limited to just about 1% [4] due to the large parasitic capacitance C_z in the PZT. The half-cycle resonance technique [2], whose operation is illustrated in the left of Fig. 23.5.2, extracts energy with the help of resonance using an external inductor and increases the amount of energy extraction by about twice.

In contrast, we can obtain energy from PZT far more than twice in the proposed method using advanced resonance technique as shown in the right of Fig. 23.5.2. In this case, the waveform continuously grows until limited by external means as LC resonance appears at every edge of the waveform. Note that the resonant period is much shorter than the AC period of the PZT material. The resonance starts by closing M1 of Fig. 23.5.1 when the voltage of the capacitor C_z reaches the peak value of V_{op} of the normal AC waveform of the PZT and the capacitor voltage is quickly inverted through the inductor. At the end of resonance, M1 is opened and the PZT current, i_{PZT} , charges C_z up again with the PZT vibration frequency until i_{PZT} reaches zero when its voltage has the next inverted peak. If this process is repeated in multiple cycles, the voltage V_z across C_z looks a square-like waveform with growing magnitude. The magnitude of V_z piles up cycle by cycle and reaches a very large value after multiple periods. This process is called the *energy pile-up mode (EPM)*, and thus we refer to the proposed scheme as *energy pile-up resonance (EPR)*. For a target magnitude of V_z in EPM, the peak value of V_z can be limited by extracting some amount of energy from the LC circuit when V_z reaches V_{Limit} and the extracted energy is transferred to the load in the form of current during the time t_{L2} by opening M1 and closing M3. This mode is called the *energy transfer mode (ETM)*. Note that the TEG operation must not interrupt the EPR operation. In order to prevent such a problem, as shown in the Fig. 23.5.1, RS, the resonance start signal, is delivered to the TEG controller to open M2 during the EPR. The “Peak Value Checker” block in Fig. 23.5.1 distinguishes whether the operation mode is EPM or ETM.

A proper control of the EPM and ETM is the crucial design point for large energy extraction. Figure 23.5.3 (bottom) shows the timing and circuit blocks for the M1

switch control in the EPR. The EPR operation starts by closing M1 when V_z hits its peak value. During the EPM, the “Full Inversion Detector” senses the voltage of C_z and opens M1 when V_{ci} reaches zero, where V_{ci} is the partial integration voltage of V_z by $(R_{i1}/R_{i2})C_i$ and represents the information of resonant current during the resonance interval. During the ETM, the “Resonance Interceptor” opens M1 when V_z hits the limit value of V_{Limit} . At this instant, V_{ci} is reset to zero by M_i to prepare for the next integration. Then, a part of the inductor energy is intercepted and transferred to the load when the mode is changed from the EPM to the ETM. The enlarged waveform illustrated at the bottom right of Fig. 23.5.3 shows that the energy transfer occurs during the period of t_{L2} . The amount of energy E_L flowing into the load during ‘ t_{L2} ’ is given by $E_L = 1/2 \cdot C_z \cdot ((V_{max} + V_{in})^2 - (V_{Limit} - V_{in})^2)$, where V_{Limit} must be set up properly considering the breakdown voltage of the CMOS process because the maximum of V_z is determined by $R_z \cdot i_{PZT}$ and it can be up to tens of volts.

To control the resonance that operates with much higher voltage V_z than V_{Load} , an attenuated signal of V_z is required. The “Sampling Attenuator and Peak Detector” shown in Fig. 23.5.3 (top) makes the attenuated signal ‘ V_{zs} ’ from V_z . For this purpose, it uses two series connected capacitors that reduces V_z by $C_1/(C_1+C_2)$. The DC level of V_{zs} is determined as $(C_3 \cdot VDD)/(C_3+C_4)$ by the capacitive voltage divider of C_3 and C_4 ($C_4=C_{41}+C_{42}$). The peak detector compares V_{zs} with its delayed signals, V_p and V_n , when the delayed signals cross over the V_{zs} , the comparator output transits and notifies the peak point. The delay circuit is designed using a capacitor and a switch-cap resistor with large equivalent resistance in small size even under a slow varying frequency of 100Hz. The small capacitors C_{42} and C_{43} in the peak detector exist to find the accurate peak point at each cycle by adding some amount of charge to C_n and removing some amount of charge from C_p , respectively. The comparator output transition is used for pulse generation in P.G whose outputs are ‘ ϕ_p ’ and ‘ ϕ_n ’ and are used for M1 control.

The top of Fig. 23.5.4 shows the detailed circuit of the “M1 Gate Driver”. The supply of the “M1 Gate Driver”, V_B , is made to be higher than the peak voltage of V_z by using V_z and V_{Load} . In order to control M1, two switches are used: M_{G1} and M_{G2} . The open state of the M1 switch is obtained by closing either M_{G1} or M_{G2} depending on the polarity of V_z . The bottom of Figure 23.5.4 shows the core circuit for the gate drivers of M_{G1} and M_{G2} to provide a negative gate diving voltage through the capacitor C_{MN} for each switch to be in the off state when turned off.

Figure 23.5.5 shows the measurement waveforms of V_z , i_L and V_{Load} when the proposed EPR operates, where the PZT is modeled as a capacitor, a resistor and a transformer. Figure 23.5.5 (top left) shows the ETM operation of the EPR when it generates 87μW output power from PZT. Considering that the conventional resonance technique [2] could achieve only 36μW output power for the same vibration amplitude, this shows an order of performance improvement. At the right of the top left of Fig. 23.5.5, the waveforms of V_z and i_L are magnified. The t_{R2} means the resonance duration between C_z and the inductor at the ETM. When the V_z meets the V_{Limit} , the resonance is intercepted and the current in the inductor flows into V_{Load} during the t_{L2} . The top right of Fig. 23.5.5 shows the transient waveform of V_z during the mode change from the EPM to the ETM. The bottom left of Fig. 23.5.5 shows that the proposed EHI charges the load from 2 to 4V with the proposed EPR. The bottom right of Fig. 23.5.5 shows the performance summary for this work. Figure 23.5.6 shows the output power increasing rate of the EPR specifically in comparison with previous designs. This shows that the available output power of EPR is controlled by V_z and reaches to 422% when the magnitude of V_z is boosted up to $7V_{pp}$ from the original PZT swing of $1.3V_{pp}$.

References:

- [1] Y. K. Ramadass and A. P. Chandrakasan, “An Efficient Piezoelectric Energy-Harvesting Interface Circuit Using a Bias-Flip Rectifier and Shared Inductor,” *ISSCC Dig. Tech. Papers*, pp. 296-297, Feb. 2009.
- [2] D. W. Kwon and G. A. Rincon-Mora, “A Single-Inductor AC-DC Piezoelectric Energy-Harvesting/Battery-Charger IC Converting $\pm(0.35$ to $1.2V)$ to $(2.7$ to $4.5V)$,” *ISSCC Dig. Tech. Papers*, pp. 494-495, Feb. 2010.
- [3] D. W. Kwon and G. A. Rincon-Mora, “A Single-Inductor $0.35\mu m$ CMOS Energy-Investing Piezoelectric Harvester,” *ISSCC Dig. Tech. Papers*, pp.78-79, Feb. 2013.
- [4] H. A. Sodano, D. J. Inman, and G. Park, “Comparison of Piezoelectric Energy Harvesting Devices for Recharging Batteries,” *Journal of Intelligent Material Systems and Structure*, vol.16, no. 10, pp. 799-807, Oct. 2005.

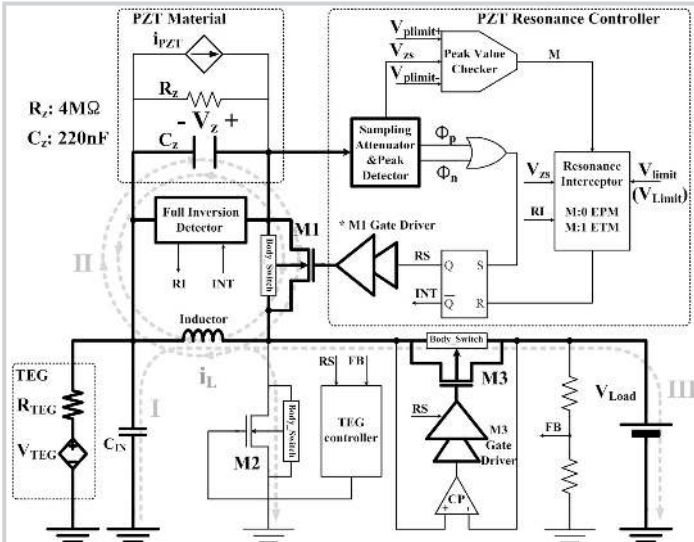


Figure 23.5.1: The proposed dual-source circuit for energy extraction from PZT material and TEG.

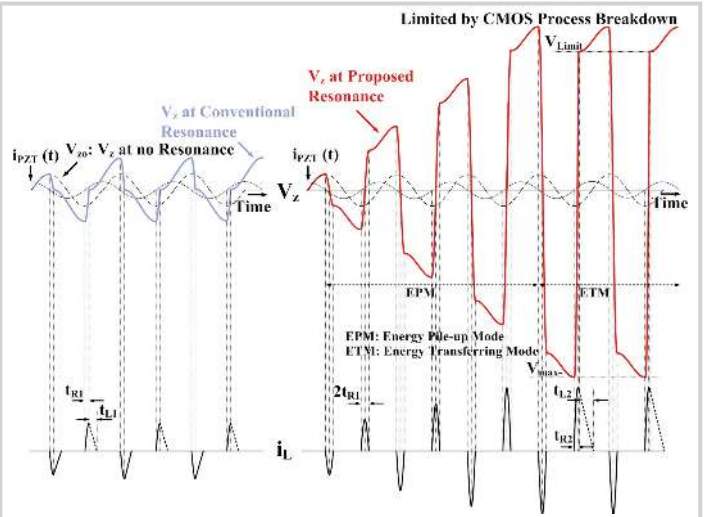


Figure 23.5.2: The conventional resonance concept (left) and the proposed Energy Pile-up Resonance concept (right) for extracting energy from the PZT material.

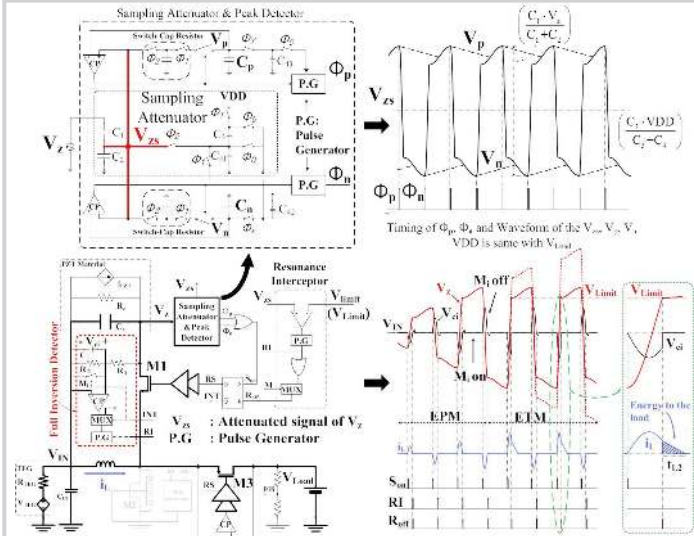


Figure 23.5.3: The full inversion detector and resonance Interceptor (bottom), and the sampling attenuator and peak detector (top).

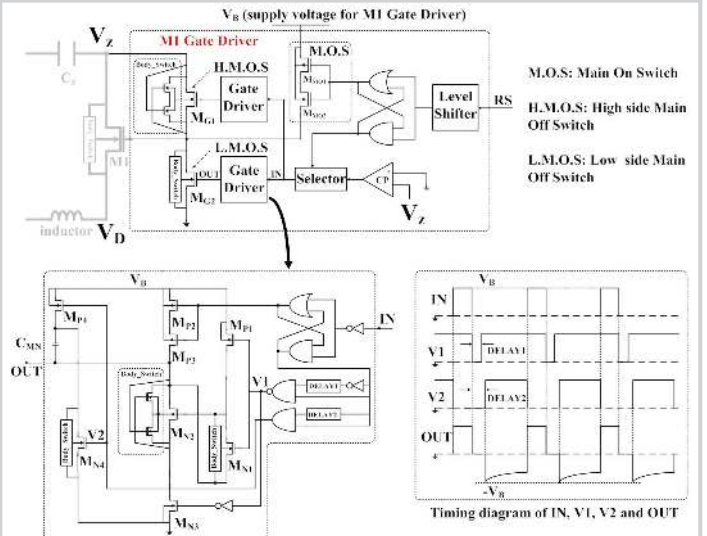


Figure 23.5.4: The proposed gate-driver scheme for M1 switch (top) and the core circuit of the gate driver (bottom).

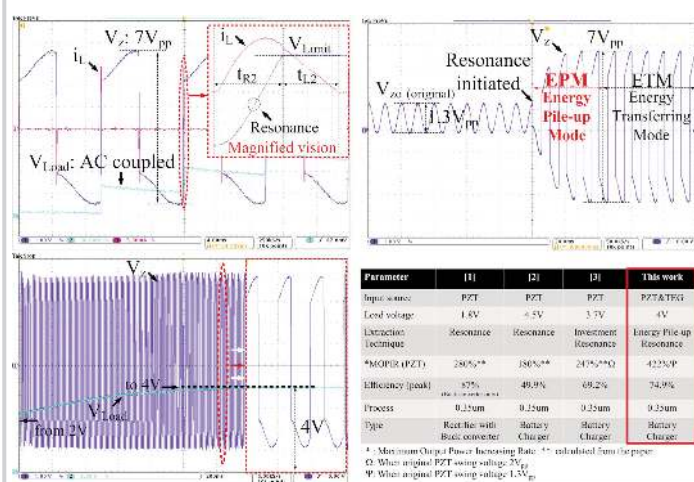


Figure 23.5.5: Measurement waveform of V_z , i_L , and V_{Load} at ETM with their magnified view (top left), mode change of V_z (top right), charging load with the proposed resonance (bottom left) and performance summary (bottom right).

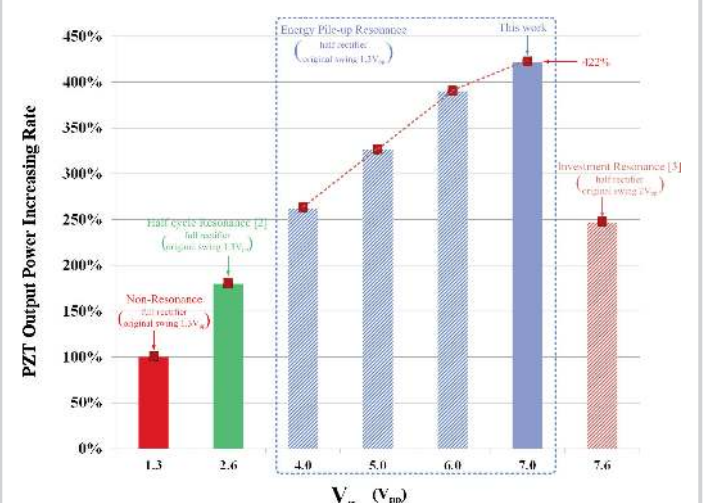


Figure 23.5.6: PZT output power increasing rate (OPIR) of energy pile-up resonance compared to previous works.

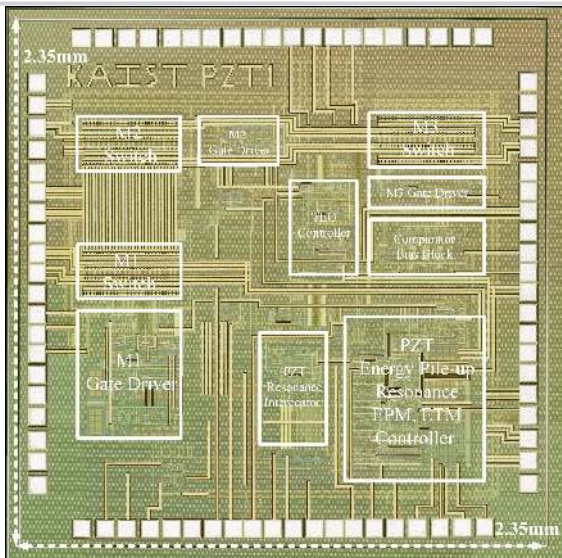


Figure 23.5.7: Chip micrograph of the proposed energy harvesting interface.